

Symmetry energy for fragmentation in dynamical nuclear collisions

Akira Ono,¹ P. Danielewicz,² W. A. Friedman,³ W. G. Lynch,² and M. B. Tsang²

¹*Department of Physics, Tohoku University, Sendai 980-8578, Japan*

²*National Superconducting Cyclotron Laboratory and Department of Physics
and Astronomy, Michigan State University, East Lansing, Michigan 48824*

³*Department of Physics, University of Wisconsin, Madison, WI 53706, USA*

(Dated: August 27, 2018)

Abstract

We extract values for the free symmetry energy as a function of the fragment size (the proton number Z) from antisymmetrized molecular dynamics (AMD) calculations of calcium collisions. Simple statistical physics describe well the distribution of hot nuclei at breakup, provided the surface symmetry term in the free energy is much smaller at high excitation than in ground state nuclei. This result may reflect the condition of low density and finite temperature when these systems disassemble.

PACS numbers: 25.70.Pq

Free energies play an important role in mixed phase environments. For nucleonic systems, such environments may be found in subsaturation density systems formed in nucleus-nucleus collisions, supernova collapses [1] and in the inner crusts of neutron stars [2, 3]. In these scenarios, the free energy of fragments largely defines the balance between denser fragments and the more dilute nucleonic gas. Key uncertainties to the prediction of free energies are their dependencies on temperature, density and isospin asymmetry. The latter uncertainty is particularly relevant to the inner crust of neutron stars, where the nuclear isospin asymmetry term stabilizes nuclear droplets enveloped by a lower density neutron gas [2, 3]. The development of experiment constraints on the asymmetry term constitutes an important scientific objective.

Here we focus on multifragmentation in nucleus-nucleus collisions. Many aspects of such data have been successfully described by equilibrium statistical models [4, 5, 6] that assume fragments to be produced by a low density phase transition that occurs during the expansion stage of a collision. The success of such descriptions suggests applications of statistical theory to such collisions may provide constraints on the free energies and their asymmetry dependence. Such comparisons provide an experimental test of the validity of equilibrium descriptions. One can also test the assumption of local thermal equilibrium by comparing the predictions of modern transport theories to equilibrium models. Calculations of isotopic observables are particularly sensitive to the degree of chemical equilibrium achieved.

We investigate these issues with the antisymmetrized molecular dynamics (AMD) code of Ref. [7]. In the present work, we analyse the yields of fragments produced in AMD simulations for central collisions of nuclei with $40 \leq A \leq 60$ at an incident energy $E/A = 35$ MeV. Even though AMD does not require the assumption of equilibrium, we have shown in a previous paper [8] that some observables obtained from predicted isotope yields, such as isoscaling, are consistent with the expectations from a statistical interpretation of fragment formation.

If the yield of fragments, produced with N neutrons and Z protons in these collisions, is governed by a statistical process at constant pressure, the fragment yield $Y(N, Z)$ can be related to the nuclear free energy $G_{\text{nuc}}(N, Z)$ by the relation

$$Y(N, Z) \propto \exp \left[-\frac{G_{\text{nuc}}(N, Z)}{T} + \frac{\mu_n}{T}N + \frac{\mu_p}{T}Z \right], \quad (1)$$

where μ_n and μ_p are the neutron and proton chemical potentials. At temperatures relevant

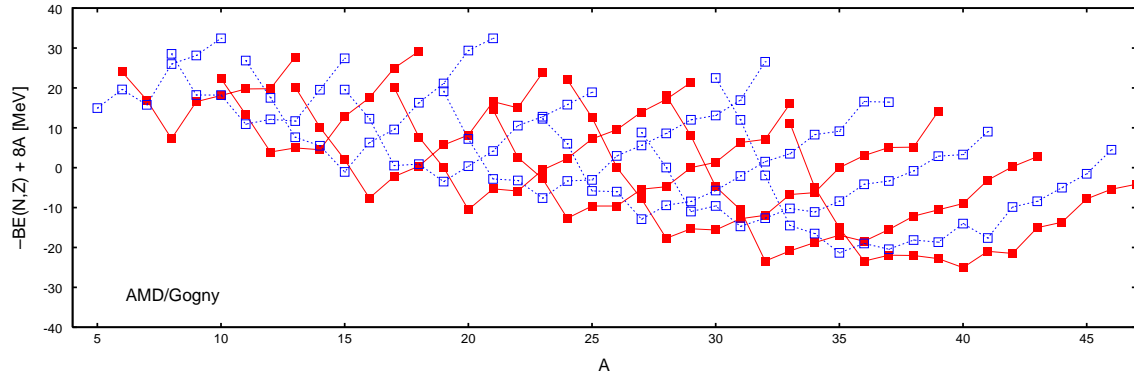


FIG. 1: Binding energies (not per nucleon) of nuclei calculated by AMD with the Gogny force. The quantities $-\text{BE}(N, Z) + 8(N + Z)$ MeV are shown by filled and open squares for even- Z and odd- Z nuclei, respectively. Lines connect isotopes.

for multi-fragmentation, the temperature dependence of the asymmetry term in the free energy for bulk nuclear matter is expected to be negligible. However, the temperature dependence of the surface symmetry term of the free energy is not well known. The present study suggests that the surface contribution to the symmetry free energy may be weakened under the conditions associated with fragment formation.

Calculations within the AMD formalism have demonstrated its capability of reproducing many quantal features of ground state nuclei [9]. The present AMD code was streamlined for collisions; it nevertheless reproduces ground state binding energies of nuclei to within about 0.5 MeV/nucleon. Figure 1 shows the binding energies of nuclei $\text{BE}(N, Z)$ with $A \lesssim 40$ which are obtained by minimizing the energy within AMD by adopting the Gogny force [10]. In order to remove the strong A -dependence, we plot $-\text{BE}(N, Z) + 8A$ MeV. We note that the free energy equals the energy itself at zero temperature and pressure, i.e. $G_{\text{nuc}}(N, Z, T = 0, P = 0) = -\text{BE}(N, Z)$.

Much of our present knowledge of the symmetry energy has been extracted by fitting the nuclear binding energies with the liquid-drop mass formula which contains a symmetry energy term such as

$$E_{\text{sym}}(N, Z) = c(A) \frac{(N - Z)^2}{A}. \quad (2)$$

In the simplest mass formula [11], the coefficient is independent of the nuclear size, $c(A) = c_{\text{sym}}$, which assumes the volume nature of the symmetry energy. On the other hand, advanced mass formulas [12, 13, 14] have introduced the A -dependence of $c(A)$ as the surface effect.

The extraction of $c(A)$ from the nuclear binding energies is not quite straightforward even for ground state nuclei. For example, if one extracts the symmetry energy by using the energy difference of neighboring nuclei [15], the symmetry energy is largely a fluctuating function in the nuclear chart due to shell and paring effects. Nevertheless, the global fitting with the assumption of $c(A) = c_v + c_s A^{-1/3}$, together with the standard volume, surface, Coulomb and paring terms, usually results in a reasonable value of the coefficients. For example, we obtain $c_v = 27.3$ MeV and $c_s = -23.7$ MeV by fitting all the available information of the binding energies of nuclei [16], while we obtain $c_v = 30.1$ MeV and $c_s = -35.1$ MeV by fitting the nuclei with $7 \leq A \leq 40$.

If we fit the AMD binding energies in Fig. 1 for $7 \leq A \leq 40$, we obtain $c_v = 30.9$ MeV and $c_s = -35.2$ MeV. The extracted value of c_v is comparable with the symmetry energy in infinite nuclear matter at saturation density ρ_0 . To a good approximation, the nuclear matter EOS at zero temperature can be written as

$$E(\rho, \delta)/A = E(\rho, \delta = 0)/A + C_{\text{sym}}(\rho)\delta^2, \quad (3)$$

where $\rho = \rho_n + \rho_p$ and $\delta = (\rho_n - \rho_p)/\rho$, and the symmetry energy coefficient has the value $C_{\text{sym}}(\rho_0) = 30.7$ MeV for the Gogny force. The present study of heavy ion fragmentation reactions will provide information about the symmetry free energy at subsaturation densities and finite temperatures.

In order to extract the symmetry free energy from Eq. (1), it is necessary to obtain the fragment yields $Y(N, Z)$ for a wide range of isotopes. This is practically impossible if we utilize the products produced in only one reaction system. However, we overcome this limitation by combining the results from various reaction systems here labeled by an index i . We calculate $^{40}\text{Ca} + ^{40}\text{Ca}$ ($i = 1$), $^{48}\text{Ca} + ^{48}\text{Ca}$ ($i = 2$), $^{60}\text{Ca} + ^{60}\text{Ca}$ ($i = 3$) and $^{46}\text{Fe} + ^{46}\text{Fe}$ ($i = 4$) collisions at zero impact parameter and an incident energy $E/A = 35$ MeV. Previous calculations with an equivalent version of AMD and the Gogny force [17, 18] reproduce experimental data for various fragment observables in $^{40}\text{Ca} + ^{40}\text{Ca}$ collisions at $E/A = 35$ MeV.

AMD represents the wavefunction of the colliding system by fully antisymmetrized products of Gaussian nucleon wave packets and propagates these wave packets microscopically during the collision [7, 17, 19]. The centroids of the nucleonic wave packets move deterministically through the mean field potential formed by the interactions with other nucleons. In

addition, the followed state of the simulation branches stochastically and successively into a huge number of reaction channels. The branching is caused by the two-nucleon collisions and by the splittings of the wave packets. The interactions are parameterized in the AMD model in terms of an effective force acting between nucleons and in terms of the two-nucleon collision cross sections. We adopt the Gogny effective force [10] in this paper.

We simulate collisions by boosting two nuclei whose centers were separated by 9 fm and calculating the dynamical evolution of each collision until $t = 300 \text{ fm}/c$. The numbers of simulated events are 1040, 949, 978 and 1400, respectively, for the four systems. In central collisions, as shown in previous papers [17, 18], the projectile and target basically penetrate each other and many fragments are formed not only from the projectilelike and targetlike parts but also from a neck region between the two parts. The nuclear matter seems to be strongly expanding one-dimensionally in the beam direction.

As we have shown in Ref. [8], the AMD results satisfy the isoscaling relation [20]

$$Y_i(N, Z)/Y_{i'}(N, Z) \propto e^{\alpha N + \beta Z} \quad (4)$$

with parameters α and β , for the fragment yields from two different reaction systems (i and i') with different neutron-to-proton ratios. When we have four reaction systems ($i = 1, 2, 3, 4$), the fragment yields $Y_i(N, Z)$ are related to the yields $Y_1(N, Z)$ of the reference system by

$$Y_1(N, Z) = Y_i(N, Z) e^{-\alpha_i N - \gamma_i(Z)}. \quad (5)$$

The yields $Y_1(N, Z)$ for one reaction system can have good statistics only in a narrow region of (N, Z) . The isoscaling relation is utilized with respect to N to extend the range of (N, Z) . We take the $^{40}\text{Ca} + ^{40}\text{Ca}$ system as the reference system and therefore $\alpha_1 = \gamma_1(Z) = 0$. The quantity $-\ln Y_1(N, Z)$, i.e. the fragment yields for $^{40}\text{Ca} + ^{40}\text{Ca}$, can be represented in four different ways by using the scaled yields for different reaction systems which have good statistics in different regions. They are combined by

$$K(N, Z) = \sum_{i=1}^4 w_i(N, Z) [-\ln Y_i(N, Z) + \alpha_i N + \gamma_i(Z)] \quad (6)$$

where the averaging weights $w_i(N, Z)$ are determined by minimizing the statistical errors in $K(N, Z)$ for individual (N, Z) . The isoscaling parameters α_i , which is common to all Z , have been obtained by the isoscaling fit [8]. The parameters $\gamma_i(Z)$ ($i = 2, 3, 4$) for each Z

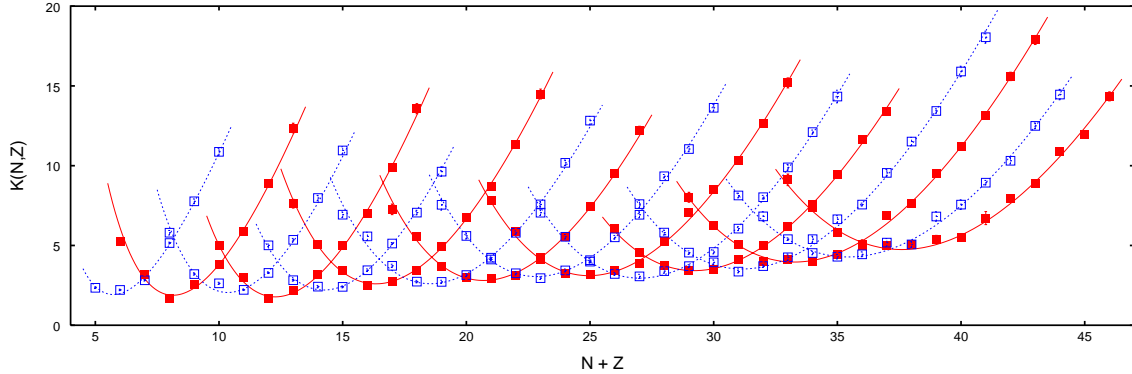


FIG. 2: The values of $K(N, Z)$ for $3 \leq Z \leq 18$ are shown by symbols for the abscissa of $N + Z$. The values are obtained by combining the results of $^{40}\text{Ca} + ^{40}\text{Ca}$, $^{48}\text{Ca} + ^{48}\text{Ca}$, $^{60}\text{Ca} + ^{60}\text{Ca}$ and $^{46}\text{Fe} + ^{46}\text{Fe}$ simulations. The error bars show the statistical uncertainty due to the finite number of events. The curve for each Z was obtained by fitting $K(N, Z)$ using Eq. (7).

are determined by optimizing the agreement of the quantities $[-\ln Y_i(N, Z) + \alpha_i + \gamma_i(Z)]$ from different reactions $i = 1, 2, 3$ and 4 .

The values of $K(N, Z)$ obtained from the AMD simulations are shown by the open and filled squares in Fig. 2 for odd- and even- Z nuclei, respectively. Even though the event numbers are not very large, $K(N, Z)$ has been obtained for a wide region of (N, Z) . In most cases $K(N, Z)$ covers more than 10 isotopes with good statistical precisions for each Z .

So far, we have not assumed any specific form of $K(N, Z)$. Nevertheless, the results show a very smooth behavior of $K(N, Z)$ as a function of N and Z . The shell and paring effects are weak in $K(N, Z)$ compared to the ground state binding energies shown in Fig. 1. Each curve in Fig. 2 shows the fitting of $K(N, Z)$ for each Z by a function

$$K(N, Z) = \xi(Z)N + \eta(Z) + \zeta(Z) \frac{(N - Z)^2}{N + Z}, \quad (7)$$

where $\xi(Z)$, $\eta(Z)$ and $\zeta(Z)$ are the fitting parameters. The result of the simulations is fitted well by this functional form. We choose the quadratic term similar to Eq. (2) for convenience, so that the parameter $\zeta(Z)$ is directly related to the symmetry energy as shown below.

The obtained values of $\zeta(Z)$ are shown in Fig. 3 by solid points. Except for light fragments ($Z \lesssim 5$), $\zeta(Z)$ is a smooth function of Z which depends on Z very weakly. Within the uncertainty in the fitting procedure, the trend does not depend on the number of reaction systems included in Fig. 2. As expected, the Z -dependence becomes more smooth and stable

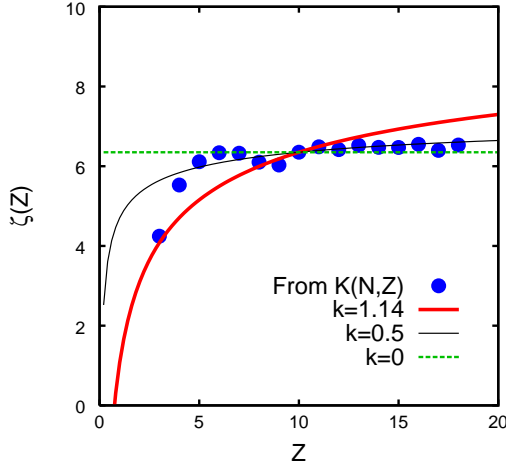


FIG. 3: The solid points are the extracted values of the coefficients $\zeta(Z)$ of Eq. (7) using the combined fragment yields of four systems shown in Fig. 2. The thick solid curve, the thin solid curve and the dashed line show functions $\zeta(Z) \propto 1 - k(2Z)^{-1/3}$ normalized at $Z = 10$ for $k = 1.14$, 0.5 and 0 , respectively.

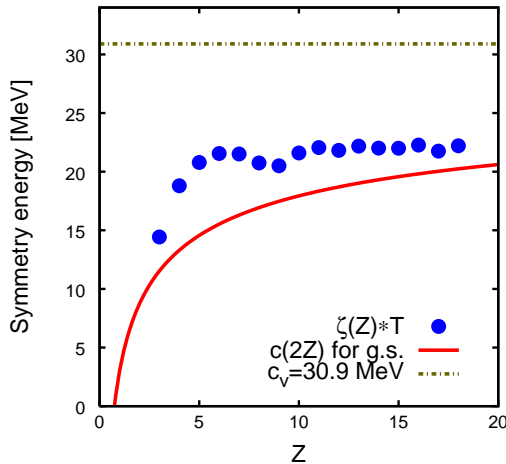


FIG. 4: The solid points show $\zeta(Z)T$ when $T = 3.4$ MeV is assumed. The dot-dashed horizontal line shows the volume symmetry energy $c_v = 30.9$ MeV for the ground state nuclei calculated with AMD. The solid line shows the symmetry energy $c(A = 2Z) = c_v + c_s(2Z)^{-1/3}$ for the ground state nuclei ($c_v = 30.9$ MeV and $c_s = -35.2$ MeV).

by including more reaction systems (up to four in the present work) due to the extension of the range of N .

Next we will show that the extracted value of $\zeta(Z)$ can be regarded as the ratio of the symmetry energy to the temperature. Under the assumption of equilibrium, $K(N, Z)$ is identified with the exponent of Eq. (1) with inverted signs. If we approximate the nuclear free energy $G_{\text{nuc}}(N, Z)$ by a smooth function of (N, Z) , $K(N, Z)$ can be written as

$$K(N, Z) = f(A, Z) + g(A) \frac{(N - Z)^2}{N + Z} + aN + bZ, \quad (8)$$

where $f(A, Z)$ and $g(A)$ have smooth A dependence. Specifically, we associate the symmetry energy $c(A)$ in $G_{\text{nuc}}(N, Z)$ with $g(A)$ by $g(A) = c(A)/T$. $f(A, Z)$ and the linear terms in N and Z can be associated with terms such as volume, surface and Coulomb terms in the free energy and the chemical potential terms in Eq. (1). Because the range of important N for each Z is limited, we can expand $f(A, Z)$ and $g(A)$ with respect to N for each Z . By denoting the typical value of A for each Z by $\bar{A}(Z)$, $f(A, Z) \approx f(\bar{A}(Z), Z) + f'(\bar{A}(Z), Z)(N + Z - \bar{A}(Z))$ and $g(A) \approx g(\bar{A}(Z))$. The higher order terms are negligible as can be checked directly by assuming the nominal values of the liquid-drop coefficients.

Thus we have shown that Eq. (7) is a natural form and that the coefficient $\zeta(Z)$ is related to the symmetry free energy $c(A)$ by

$$\zeta(Z) = c(\bar{A}(Z))/T. \quad (9)$$

In principle, $\zeta(Z)$ could depend on Z , reflecting the size-dependence of the symmetry energy $c(A)$. However, the extracted values of $\zeta(Z)$ in Fig. 3 are almost independent of Z for $Z \gtrsim 5$. This suggests a reduction of the surface contribution to the symmetry energy. The three curves in Fig. 3 show functions $\zeta(Z) \propto 1 - k(2Z)^{-1/3}$ for different surface-to-volume ratios $k = 1.14$ (thick solid line), 0.5 (thin solid line) and 0 (horizontal dashed line), respectively. The curves are normalized at $Z = 10$. The Z -dependence of $\zeta(Z)$ cannot be explained by the surface-to-volume ratio $k = -c_s/c_v = 1.14$ for the symmetry energy of ground state nuclei. The result shows that the surface effect in $\zeta(Z)$ is reduced to between $k = 0$ and 0.5 .

There can be several possible explanations for the weakening of the surface symmetry free energy. First of all, it is not very surprising that the coefficient in the free energy at a finite temperature is different from that at the zero temperature. As is well known, the surface tension reduces towards zero when the temperature is raised towards the critical

temperature. A similar effect has been obtained for the symmetry free energy in Thomas-Fermi surface calculations [21, 22]. If we adopt the formula in Ref. [21], the reduction factor of the surface symmetry energy is approximately $[1 - (T/T_c)^2]^2 = 0.91$ for $T = 3.4$ MeV (see below) and the critical temperature $T_c = 16$ MeV. This reduction is, however, not sufficient to explain the weak Z -dependence of $\zeta(Z)$. Another explanation may be associated with the fact that fragments are not isolated when they are formed. When the density fluctuation is developing from a uniform low density matter, the fragments are still interacting with attractive force through their surfaces. Therefore, surface free energies could be expected to be smaller for these fragments than for totally isolated fragments. Independent of the physical origin for the weakening of the surface symmetry free energy, it suggests that the volume quantity, which is the same as that in the infinite nuclear matter, can be directly obtained by the analysis of the fragmentation results even though the produced fragments are not very large.

In the above analysis, only the ratio of the symmetry free energy to the temperature is obtained. In the present theoretical approach, it is possible to get the density and the temperature by studying the response of the results to a change of the symmetry term in the effective force. In Ref. [8] we have derived the density $\rho \sim 0.08 \text{ fm}^{-3}$ and the temperature $T \sim 3.4 \text{ MeV}$ for the same reaction systems studied in the present paper. This result is consistent to the idea that the fragments are formed in a low density nuclear matter at a finite temperature. The solid points in Fig. 4 show $\zeta(Z)T$ so that the extracted $\zeta(Z)$ can be directly compared to the symmetry energy. The value of the symmetry energy extracted from fragmentation is significantly lower than that of the bulk nuclear matter at normal nuclear matter density, $C_{\text{sym}}(\rho_0) \approx c_v = 30.9 \text{ MeV}$ shown by the dot-dashed horizontal line in Fig. 4, and this must be due to the reduced density, $\rho \sim 0.08 \text{ fm}^{-3} < \rho_0$.

The solid line in Fig. 4 shows the symmetry energy $[30.9 - 35.2(2Z)^{-1/3}] \text{ MeV}$ that has been obtained by fitting the ground state binding energies calculated with AMD. The extracted symmetry energy is smaller than the ground state symmetry energy probably because of the greater reduction from the surface contribution when fragments are formed.

In conclusion, we have analysed AMD simulation results from nuclear collisions of various nuclei with different neutron-to-proton ratios. Fragment yields from different reaction systems are combined using the isoscaling relation. The availability of fragment yields over a wide range of N and Z allows us to extract the symmetry energy at low density when

fragments are formed. The results are consistent to the idea that the fragments are formed in nuclear matter at a low density and at a finite temperature. The extracted symmetry energy shows almost no surface effect in it, which suggests that the property of infinite nuclear matter can be directly obtained from the information of fragmentation.

Acknowledgments

This work was supported by Japan Society for the Promotion of Science and the US National Science Foundation under the U.S.-Japan Cooperative Science Program (INT-0124186), by the High Energy Accelerator Research Organization (KEK) as a Supercomputer Project, and by grants from the US National Science Foundation, PHY-0245009, PHY-0070161 and PHY-01-10253, and a Grant-in-Aid for Scientific Research from the Japan Ministry of Education, Science and Culture. The work was also partially supported by RIKEN as a nuclear theory project.

- [1] H.A. Bethe, *Rev. Mod. Phys.* **62**, 801 (1990).
- [2] C.J. Pethick and D.G. Ravenhall, *Ann. Rev. Nucl. Part. Sci.* **45**, 429 (1995).
- [3] J.M. Lattimer and M. Prakash, *Ap. J.*, **550**, 426 (2001).
- [4] D.H.E. Gross, *Phys. Rep.* **279**, 119 (1997).
- [5] J.P. Bondorf, A.S. Botvina, A.S. Iljinov, I.N. Mishustin, and K. Sneppen, *Phys. Rep.* **257**, 133 (1995).
- [6] W. P. Tan, S. R. Souza, R. J. Charity, R. Donangelo, W. G. Lynch, and M. B. Tsang, *Phys. Rev. C* **68**, 034609 (2003).
- [7] A. Ono, *Phys. Rev.* **C59**, 853 (1999).
- [8] A. Ono, P. Danielewicz, W.A. Friedman, W.G. Lynch and M.B. Tsang, *Phys. Rev. C* **68**, 051601(R) (2003).
- [9] Y. Kanada-En'yo, M. Kimura, and H. Horiuchi, *C. R. Physique* **4**, 497 (2003), and references therein.
- [10] J. Dechargé and D. Gogny, *Phys. Rev.* **C21**, 1568 (1980).
- [11] C. F. V. Weizsäcker, *Z. Physik* **96**, 431 (1935).

- [12] W. D. Myers and W. J. Swiatecki, Nucl. Phys. **A81**, 1 (1966).
- [13] P. Möller, J. R. Nix, W. D. Myers and W. J. Swiatecki, At. Data Nucl. Data Tables **59**, 185 (1995).
- [14] P. Danielewicz, Nucl. Phys. **A727**, 233 (2003).
- [15] J. Jänecke, T. W. O'Donnell, V. I. Goldanskii, Nucl. Phys. **A728**, 23 (2003).
- [16] G. Audi and A. H. Wapstra, Nucl. Phys. A595, 409 (1995).
- [17] A. Ono and H. Horiuchi, Phys. Rev. **C53**, 2958 (1996).
- [18] R. Wada, K. Hagel, J. Cibor, J. Li, N. Marie, W. Q. Shen, Y. Zhao, J. B. Natowitz and A. Ono, Phys. Lett. **B422**, 6 (1998).
- [19] A. Ono, H. Horiuchi, Toshiki Maruyama and A. Ohnishi, Phys. Rev. Lett. **68**, 2898 (1992); A. Ono, H. Horiuchi, Toshiki Maruyama and A. Ohnishi, Prog. Theor. Phys. **87**, 1185 (1992).
- [20] H. S. Xu, M. B. Tsang, T. X. Liu, X. D. Liu, W. G. Lynch, W. P. Tan, A. Vander Molen, G. Verde, A. Wagner, H. F. Xi, C. K. Gelbke, L. Beaulieu, B. Davin, Y. Larochelle, T. Lefort, R. T. de Souza, R. Yanez, V. E. Viola, R. J. Charity and L. G. Sobotka, Phys. Rev. Lett. **85**, 716 (2000); M. B. Tsang, W. A. Friedman, C. K. Gelbke, W. G. Lynch, G. Verde and X. S. Xu, Phys. Rev. Lett. **86**, 5023 (2001).
- [21] J. M. Lattimer and F. D. Swesty, Nucl. Phys. **A535**, 331 (1991).
- [22] D. G. Ravenhall, C. J. Pethick and J. M. Lattimer, Nucl. Phys. A407, 571 (1983).